The Journal of Immunology

RESEARCH ARTICLE | OCTOBER 01 2001

An Atypical Population of NK Cells That Spontaneously Secrete IFN-γ and IL-4 Is Present in the Intraepithelial Lymphoid Compartment of the Rat[1,2]

Derrick J. Todd; ... et. al

J Immunol (2001) 167 (7): 3600–3609.
https://doi.org/10.4049/jimmunol.167.7.3600

An Atypical Population of NK Cells That Spontaneously Secrete IFN-γ and IL-4 Is Present in the Intraepithelial Lymphoid Compartment of the Rat[1,2]

Derrick J. Todd, Dale L. Greiner, Aldo A. Rossini, John P. Mordes, and Rita Bortell[3]

The intestinal lymphoid compartment of the rat is large and diverse, but the phenotype and functions of its constituent cell populations are not fully characterized. Using new methodology for the isolation and purification of rat intestinal intraepithelial lymphocytes (IELs), we previously identified a population of $\alpha\beta$- and $\gamma\delta$-TCR$^-$ NKR-P1A$^+$ NK cells. These cells were almost completely restricted to the CD4$^-$CD8$^-$ IEL population, and unlike peripheral NK cells in the rat, they were CD2$^-$. We now report that rat intraepithelial NK (IENK) and peripheral NK cells are similar in morphology, in their ability to lyse NK-sensitive targets, and in their ability to suppress a one-way mixed lymphocyte culture. In contrast, however, intraepithelial and splenic NK cells differ markedly in two respects. First, IENK cells express high levels of ADP-ribosyltransferase 2 (a marker of regulatory T cells in the rat) and CD25, whereas peripheral NK cells do not. Second, unlike splenic NK cells, a substantial fraction of IENK cells appear to spontaneously secrete IL-4 and/or IFN-γ. We conclude that the rat IEL compartment harbors a large population of NKR-P1A$^+$CD3$^-$ cells that function as NK cells but display an activated phenotype and unusual cytokine profile that clearly distinguish them from splenic NK cells. Their phenotypic and functional characteristics suggest that these distinctive IENK cells may participate in the regulation of mucosal immunity. *The Journal of Immunology,* **2001, 167: 3600–3609.**

The intestine is the largest lymphoid organ in the body, challenged constantly by an enormous quantity and diversity of Ags. The intestinal lymphoid compartment is not only large but also very diverse, and the phenotype and functions of its constituent cell populations are not fully characterized (1). In addition, mucosal lymphoid tissues appear to be regulated by unique mechanisms that govern highly specialized processes such as oral tolerance and controlled (or physiologic) chronic inflammation. Defects in the function of intestinal immune system regulation have been associated with celiac disease (2) and inflammatory bowel diseases (3–5). In addition, there are specialized lymphoid populations, in particular intraepithelial T lymphocytes (6), that respond to alternative pathways of activation. Coupled with the specialized Ag-presenting capabilities of intestinal epithelial cells (7), these lymphoid populations are thought to participate in immune responses that are under the control of distinct, but as yet poorly characterized, regulatory factors (1).

Using new methodology for the isolation and purification of rat intestinal intraepithelial lymphocytes (IEL),[4] we previously identified a population of $\alpha\beta$- and $\gamma\delta$-TCR$^-$NKR-P1A$^+$ intraepithelial NK (IENK) cells (8). These cells were almost completely restricted to the CD4$^-$CD8$^-$ IEL population, and unlike peripheral NK cells in the rat, they were CD2$^-$. We now report the phenotypic and functional characteristics of these IENK cells. The data suggest that the rat IEL compartment harbors a large population of NKR-P1A$^+$CD3$^-$ cells that function as NK cells, but display an activated phenotype and an unusual cytokine profile that clearly distinguish them from splenic NK cells. Their phenotypic and functional characteristics suggest that these distinctive IENK cells may participate in the regulation of mucosal immunity.

Materials and Methods

Animals

Wistar Furth (WF), Dark Agouti (DA), and Brown Norway (BN) rats of both sexes were obtained from Harlan Sprague Dawley (Indianapolis, IN). Additional WF rats of both sexes were obtained from Charles River Laboratories (Wilmington, MA). All animals were certified to be serologically free of Sendai virus, pneumonia virus of mice, sialodacryoadenitis virus, rat corona virus, Kilham rat virus, H1 (Toolan's virus), mouse poliovirus (GD7), Reo-3, *Mycoplasma pulmonis*, lymphocytic choriomeningitis virus, mouse adenovirus, Hantaan virus, and *Encephalitozoon cuniculi*. All animals were housed in a viral Ab-free facility until used and maintained in accordance with recommendations in the *Guide for the Care and Use of Laboratory Animals* (Institute of Laboratory Animal Resources, National Research Council, National Academy of Sciences, 1996) and the guidelines of the institutional animal care and use committee of the University of Massachusetts Medical School.

Abs and recombinant cytokines

For flow microfluorometry, fluorochrome- or biotin-conjugated mAbs directed against NKR-P1A (clone 10/78), CD2 (clone OX-34), CD3 (clone G4.18), CD5 (clone OX-19), CD8α (OX-8), CD25 (IL-2R α-chain, clone OX-39), CD28 (clone JJ319), CD45RC (clone OX-22), CD54 (ICAM-1, clone 1A29), and $\alpha\beta$-TCR (clone R73) were obtained from BD PharMingen (San Diego, CA). The hybridoma secreting the 6A5 rat anti-rat ADP-ribosyltransferase 2b (ART2b)[5] (IgG1) mAb is maintained in our laboratory (8).

Department of Medicine, University of Massachusetts Medical School, Worcester, MA 01605

Received for publication February 21, 2001. Accepted for publication July 25, 2001.

The costs of publication of this article were defrayed in part by the payment of page charges. This article must therefore be hereby marked *advertisement* in accordance with 18 U.S.C. Section 1734 solely to indicate this fact.

[1] This work was supported in part by a grant from the Iacocca Foundation (to R.B.), a Medical Scholars Award from the American Diabetes Association (to D.J.T.), Diabetes and Endocrinology Research Center Grant DK32520, and Grants DK25306, DK49106, and DK36024 from the National Institutes of Health.

[2] The contents of this publication are solely the responsibility of the authors and do not necessarily represent the official views of the National Institutes of Health.

[3] Address correspondence and reprint requests to Dr. Rita Bortell, Diabetes Division, University of Massachusetts Medical School, Two Biotech, Suite 218, 373 Plantation Street, Worcester, MA 01605. E-mail address: rita.bortell@umassmed.edu

[4] Abbreviations used in this paper: IEL, intraepithelial lymphocytes; ART, ADP-ribosyltransferase; IENK, intraepithelial NK; IE-T cell, intraepithelial T cell; MLN, mesenteric lymph node; TNP, trinitrophenol.

[5] A new nomenclature for the rat has been adopted. ART2 now replaces RT6; ART2b, an isoform of ART2, now replaces RT6.2 (29).

0022-1767/01/$02.00

For measurement of IL-4-secreting cells by ELISPOT, paired mAbs (purified OX-81 and biotinylated B11-3) directed against IL-4 were obtained from BD PharMingen. For measurement of IFN-γ by ELISPOT, the capture mAb (clone DB-1) was obtained from BioSource International (Camarillo, CA), and the detection rabbit anti-rat IFN-γ polyclonal Ab was obtained from Torrey-Pines Biolabs (La Jolla, CA) and biotinylated as previously described (9). Isotype control mouse IgG1, mouse IgG2a, mouse IgG3, secondary Ab (anti-rat IgG1), alkaline phosphatase-conjugated streptavidin, and CyChrome-conjugated streptavidin were purchased from BD PharMingen. HRP-conjugated avidin D was purchased from Vector Laboratories (Burlingame, CA). Recombinant rat IL-2, IFN-γ, and IL-4 were purchased from R&D Systems (Minneapolis, MN).

Cell preparation

IEL were prepared from rat small intestine using previously described methods with minor modifications (8). Briefly, the entire small intestine was gently flushed with cold RPMI 1640 (Life Technologies, Grand Island, NY) to remove lumenal contents and then incubated in ice-cold RPMI 1640 for 60–120 min to delaminate epithelial cells and IEL from the basement membrane. Detached cells were recovered by flushing the intestine twice with a total of 50 ml of HEPES-buffered HBSS medium containing 1 mM dithioerythritol (Sigma, St. Louis, MO) and 10% Fetalclone I (a defined neonatal bovine serum; HyClone Laboratories, Logan, UT) at 37°C. IEL were then purified by Percoll density gradient centrifugation, and viable cells exhibiting lymphoid morphology were quantified by the method of trypan blue using a hemocytometer.

Thymi, spleens, and mesenteric lymph nodes (MLN) were removed from rats killed in an atmosphere of 100% CO_2. Single-cell suspensions were prepared by gentle extrusion through stainless steel sieves into medium consisting of cold RPMI 1640 supplemented with 5% Fetalclone I as previously described (8, 10). Spleen cell preparations were washed in medium, and erythrocytes were lysed in a hypotonic buffer (0.15 M NH_4Cl, 1.0 mM $KHCO_3$, and 0.1 mM Na_2EDTA, pH 7.4). For cytotoxicity assays, erythrocyte-depleted splenocytes were suspended in medium and adsorbed against polystyrene plates for 1 h at 37°C, and nonadherent spleen cells were recovered by gentle rinsing of the plates with ice-cold medium.

Flow microfluorometry

One-, two-, and three-color flow microfluorometric analyses were performed as previously described (8). Briefly, 1×10^6 viable splenocytes or IEL were suspended in ice-cold FACS medium (isotonic PBS supplemented with 1% Fetalclone I) and reacted with a mixture of 6A5 anti-ART2b mAb and/or biotin-conjugated Abs for 30 min at 4°C. Cells were then washed with FACS medium, reacted with FITC- and PE-conjugated Abs and/or CyChrome-conjugated streptavidin for 30 min at 4°C, washed with FACS medium, and fixed with 1% paraformaldehyde in PBS. FITC-, biotin-, and PE-conjugated isotype control Igs were used for all analyses. Cells were analyzed using a FACScan instrument (BD Biosciences, Mountain View, CA). Lymphoid cells were identified by their forward and side light scatter profiles.

IEL and splenocyte subpopulations were purified by flow microfluorometry. Freshly isolated IEL and splenocytes were reacted either with FITC-conjugated Abs directed against NKR-P1A or with FITC- and PE-conjugated Abs directed against NKR-P1A and CD3, respectively, and sorted by FACScan. As documented in Fig. 1 for one representative sample, the purity of all sorted IEL populations was >95%. The purity of sorted splenic T and NK cell populations was also documented by flow microfluorometry to be >97%. The percentage of contaminating NKR-P1A$^+$ CD3$^+$ (NK T) cells was consistently very low (<0.1%) in the sorted cell populations in all experiments.

Morphology

Purified preparations of IEL and splenocyte subpopulations were suspended in isotonic PBS and spun onto glass slides using a Shandon Cytospin 2 (Shandon, Pittsburgh, PA). Cells were reacted with Wright-Giemsa stain and evaluated by light microscopy by a qualified pathologist.

Cytotoxicity assay

Cytotoxic activity of lymphoid populations was measured using a previously described ^{51}Cr release microcytotoxicity assay with minor modifications (11). NK-sensitive YAC-1 virus-induced mouse T cell lymphoma (12) and NK-resistant C58NT(D) (13) target cells were obtained from the American Type Culture Collection (Manassas, VA) and maintained in our laboratory in AIM-V medium (Life Technologies) supplemented with 2.2×10^{-5} M 2-ME. Target cells in growth phase were labeled with ^{51}Cr as sodium chromate (150 μCi/million cells; New England Nuclear, Boston, MA), and 1.0×10^4 ^{51}Cr-labeled cells were added to each well of a 96-well microtiter plate. Unfractionated IEL, purified subpopulations of IEL, and adherent-cell-depleted splenocytes were added at E:T cell ratios ranging from 75:1 to 3:1, and the plates were incubated for 4 h at 37°C in a humidified atmosphere of 95% air-5% CO_2. All assays were performed in triplicate and averaged.

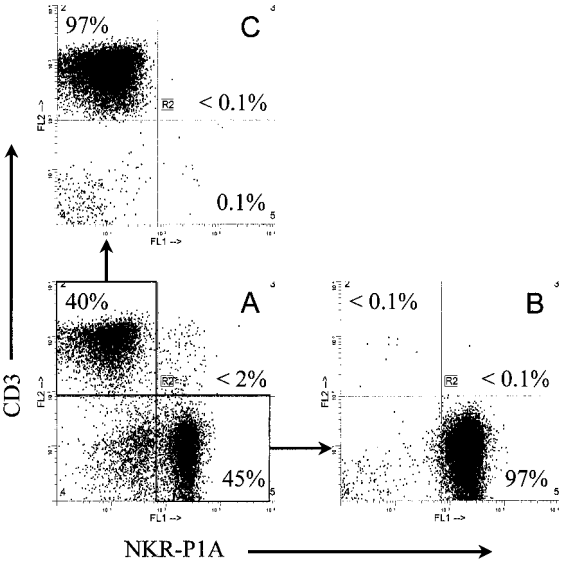

FIGURE 1. Purity of sorted IENK cells. IEL were isolated from 4- to 8-wk-old WF rats, reacted with anti-NKR-P1A and anti-CD3 mAbs (*A*), and sorted by flow microfluorometry using the indicated gates into NKR-P1A$^+$CD3$^-$ (*B*) and NKR-P1A$^-$ CD3$^+$ (*C*) populations as described in *Materials and Methods*. The percentages of purified NKR-P1A$^+$CD3$^-$ IENK cells and NKR-P1A$^-$CD3$^+$ T cells, as indicated, were very high. Shown is the result of a single representative experiment. Comparable purity was achieved in all sorts of both IEL and splenocytes used as part of subsequent experiments.

Total releasable radioactivity ($cpm_{maximal}$) was determined by incubating an aliquot of ^{51}Cr-labeled target cells with 1% Triton X-100. After incubation, cells were pelleted by centrifugation, and 100-μl aliquots of supernatant were transferred to a separate microtiter plate containing 100 μl Optiphase Supermix β-scintillation fluid (Wallac, Gaithersburg, MD) and counted (cpm_{test}) using a 1450 Microbeta Trilux instrument (Wallac). In all assays reported here, release of ^{51}Cr in the absence of effector cells ($cpm_{spontaneous}$) was <12% and <22% of the total ^{51}Cr release for YAC-1 and C58NT(D) cells, respectively. Specific cytotoxicity was calculated as a percentage using the raw counts per minute and the formula: specific lysis (%) = $((cpm_{test} - cpm_{spontaneous})/(cpm_{maximal} - cpm_{spontaneous})) \times 100\%$.

Suppressor cell assays: MLC

Inhibition of peripheral T lymphocyte proliferation by syngeneic WF IEL was measured in a one-way MLC. Responder cells were WF rat MLN cells. Stimulator cells were either syngeneic WF (RT1^u) thymocytes or allogeneic DA (RT1^a) or BN (RT1^n) thymocytes. Stimulator thymocytes were given 2 Gy of γ-radiation (~0.1 Gy/min) using a ^{137}Cs source (Gammacell 40; Atomic Energy of Canada, Ottawa, Canada). Assays were performed in 96-well plates incubated at 37°C in a final volume of 200 μl supplemented AIM-V medium in a humidified atmosphere of 95% air-5% CO_2. In preliminary experiments it was determined that optimal MLN cell proliferation in the absence of IEL was obtained after 5 days of incubation using 4.0×10^5 responder cells and 8.0×10^5 allogeneic stimulator cells. Unfractionated IEL and purified subpopulations of IEL syngeneic to the responder cells were added to cultures at IEL:responder cell ratios ranging between 1:400 and 2.5:1. [^{3}H]Thymidine (1 μCi/well; New England Nuclear) was added to each well for the final 18–24 h of culture, and total incorporation of [^{3}H]thymidine into DNA was determined as previously described (14). Radioactivity was measured using a 1450 Microbeta Trilux instrument (Wallac). All assays were performed in triplicate and averaged. The extent of suppression was calculated as a percentage using the raw counts per minute and the formula: % suppression = $(1 - ((cpm_{test\ allo} - cpm_{test\ syn})/(cpm_{max\ allo} - cpm_{max\ syn})) \times 100\%$, where $cpm_{test\ allo}$ are counts from the incubation of IEL, responder, and allogeneic stimulator

cells; $cpm_{test\ syn}$ are counts from incubation of IEL, responder, and syngeneic stimulator cells; $cpm_{max\ allo}$ are counts from the incubation of responder and allogeneic stimulator cells only; and $cpm_{max\ syn}$ are counts from the incubation of responder and syngeneic stimulator cells.

Transwell assay

To determine whether a soluble factor mediated IEL-induced suppression, MLC were performed using 24-well Costar Transwell plates (3 μm pore diameter, Fisher Scientific, Pittsburgh, PA). Responder WF MLN cells were incubated in PBS (5.0×10^7 cells/ml) containing 1 μM CFSE for 15 min at 37°C as previously described (15). After labeling, responder cells were incubated with stimulator thymocytes from syngeneic WF or allogeneic DA or BN rats prepared as described above, with 1.0×10^6 WF responder cells and 3.2×10^6 stimulator cells placed in the lower chamber of each test well. IEL from 5- to 7-wk-old WF rats (2.0×10^5 cells) were added to either the lower chamber or the upper insert chamber of test wells. Cell mixtures were cultured in supplemented AIM-V medium at a final volume of 800 μl/well. Plates were incubated at 37°C for 5 days in a humidified atmosphere of 95% air-5% CO_2. After harvest, the intensity of the intracellular CFSE signal in viable lymphocytes was measured by flow microfluorometry and used as an index of cell proliferation as previously described (16). The absolute number of mitotic events that had occurred per 10^4 responder cells in the analysis was calculated using the method of Wells et al. (17).

ELISPOT analyses

IFN-γ and IL-4 production was first measured using a previously described ELISPOT assay with minor modifications (18, 19). Briefly, 96-well Nunc Maxisorp plates (Fisher Scientific) were incubated overnight at 4°C with coating Abs (1 μg/well) diluted in sterile PBS. Plates were washed once with PBS (4°C) and blocked for 1–2 h with PBS containing 4% BSA (w/v). Plates were then washed once with PBS at 4°C, cells to be assayed were suspended in supplemented AIM-V medium and 100 μl of the cell suspension was added to each well. The optimal number of IEL assayed per well was determined in preliminary experiments and varied from 1 to 9×10^4. The optimal number of splenocytes assayed per well was also determined in preliminary experiments and varied from 1 to 52×10^4. For all ELISPOT analyses, plates were incubated at 37°C in a humidified atmosphere of 95% air-5% CO_2 for 20–24 h in the absence of additional stimulation except as noted. Stimuli included recombinant rat IL-2 (10 or 6000 U/ml) or the combination of PMA (5 ng/ml) and ionomycin (0.4 μg/ml). After incubation, culture medium was decanted, and distilled H_2O containing 0.05% Tween 20 was added to the wells for 5–10 min to lyse the cells. Plates were then washed five times with PBS/0.05% Tween 20 using an Ultrawash Plus plate washer (Dynatech, Burlington, MA). Biotinylated detection Abs (0.5 μg/well diluted with PBS containing 1% BSA) directed against IL-4 and IFN-γ or an irrelevant Ag (trinitrophenol, TNP) were then added to test wells. Plates were agitated on a plate shaker at room temperature for 60–120 min and then washed five times with PBS-0.05% Tween 20.

Next, 100 μl of a 1/1000 dilution of alkaline phosphatase-conjugated streptavidin in PBS containing 1% BSA was added to each well. Plates were again agitated at room temperature for 60–120 min, washed 10 times with PBS-0.05% Tween 20, and then washed once with PBS alone. A solution of 0.6% agarose (w/v, type VII low gelling temperature; Sigma) containing 0.1 M 2-amino-2-methyl-1-propanol (Sigma), 16.2 mM $MgCl_2$, 0.008% Triton X-405 (v/v; Sigma), and 2.3 mM 5-bromo-4-chloro-3-indolyl phosphate (Sigma) was preheated to 42°C and layered onto the plates, which were then incubated overnight at 37°C in a humidified atmosphere of 95% air-5% CO_2. The number of discrete spots visible in each well was counted using a light microscope at ×2 power. Each cytokine assay was performed using four wells, three of which were assayed using the cytokine-specific developing Ab and one of which was assayed using the irrelevant biotinylated control Ab. For analysis, the number of spots observed in the control well for each quadruplicate assay was subtracted from the number of spots counted in each of the three test wells. The maximum number of spots observed in any control well was three. The adjusted number of spots present in each of the test wells was then averaged. To account for the various numbers of cells added per well, data have been normalized to numbers of spots per 10^4 cells.

Quantification of cytokine production by cell-ELISA

The amount of IFN-γ and IL-4 secreted by IEL was quantified using a modification of the cell-ELISA (20), which is designed to avoid artifact influenced by the consumption of the cytokines that are secreted by cultured cells. For these assays, unstimulated unsorted, sorted, and remixed IEL ($1–5 \times 10^4$/well) were processed exactly as detailed in the first paragraph of the ELISPOT method described above (through the end of the culture, addition of biotinylated Abs, and washes). For quantification, additional wells were prepared in the same way at the same time, but graded amounts of IFN-γ or IL-4 instead of cells were added to these wells. Threefold dilutions of cytokine were added to wells in amounts that ranged from 1.2 to 900 pg for IFN-γ and from 0.1 to 33.3 pg for IL-4.

After the incubation, addition of detection Abs directed against IL-4 and IFN-γ or TNP and washes, 100 μl of a 1/2500 dilution of HRP-conjugated avidin D in PBS containing 1% BSA was added to each well. Plates were agitated at room temperature for 60–120 min, washed 10 times with PBS-0.05% Tween 20, and then washed once with PBS alone. Next, 100 μl of a solution containing 0.05 M Na_2HPO_4, 0.025 M sodium citrate, 1 mg/ml *o*-phenylenediamine (Sigma), and 1 μl/ml 30% (v/v) H_2O_2 was added to each test well, and plates were incubated at room temperature for 5–10 min. The reaction was stopped by adding 25 μl of 3 N HCl to each well, and absorbance at 790 nm was measured using a microplate reader (model 3550; Bio-Rad, Hercules, CA). Each IEL population (unsorted, sorted, remixed) was assayed in six wells, of which three were developed using the cytokine-specific Ab and three with the anti-TNP Ab. Each standard was assayed in three wells that were developed using the cytokine-specific Ab.

For wells to which the cytokine alone had been added, a standard curve was generated by linear regression using the software supplied with the plate reader (Microplate Manager PC, version 4.0, Bio-Rad). Curves for both IFN-γ and IL-4 were linear in the region of interest ($r > 0.98$ for each assay). The amount of cytokine present in each well that had been incubated with IEL was determined by the software. Because the cytokines produced in the course of the ELISPOT were captured and not degraded, the data are presented as picograms of cytokine produced per 10^4 cells per 24 h. No cytokine was detected in wells that were developed with the TNP-specific detection Ab or in wells to which neither cells nor cytokines had been added.

Statistical analysis

Parametric data are presented as the arithmetic mean ± SD, except in figures depicting the results of a single experiment performed in triplicate or quadruplicate. In those instances the result is shown as the mean ± SEM. Pairs of means were compared using two-tailed *t* tests with separate variance estimates and the Bonferroni adjustment for multiple comparisons as required (21, 22).

Results

The relative percentage of NKR-P1A$^+$ cells in the intraepithelial compartment of rats decreases with age

In a preliminary experiment IEL were isolated from WF rats of different ages, and the percentage of NKR-P1A$^+$ cells present was measured by flow cytometry. As shown in Fig. 2, the percentage of NKR-P1A$^+$ cells present in the IEL compartment declined with age, decreasing from ~50% in weanling rats to ~17% in retired breeder rats >16 wk old. At certain time points, the percentages of NKR-P1A$^+$ CD3$^+$ or NKR-P1A$^+$ $\alpha\beta$-TCR$^+$ (NK T) cells present in the IEL compartment were also measured and were consistently <2% (Fig. 2). The absolute number of IENK cells was determined at two time points. We observed that the yield of IEL from 4- to 6-wk-old rats was $5.1 \pm 1.9 \times 10^6$/rat ($n = 7$), of which an average of about 2.5×10^6 were IENK cells. The yield of IEL from much larger rats >16 wk old was $27.2 \pm 6.4 \times 10^6$/rat ($n = 11$), of which an average of about 5×10^6 were IENK cells. Except as noted, rats 4- to 8-wk old were used in subsequent experiments.

Intraepithelial and splenic NKR-P1A$^+$ CD3$^-$ NK cells express different cell surface Ags

It is known that intraepithelial and splenic NK cells differ with respect to the expression of at least two cell surface Ags. The majority of splenic NK cells express CD2 and CD8α, whereas <10% of IENK cells express these surface Ags (8, 23). To investigate whether intraepithelial and splenic NKR-P1A$^+$ CD3$^-$ NK cells differ phenotypically in other respects, we measured the expression of a panel of cell surface Ags on both populations. Using 7-wk-old WF rats, we confirmed that the percentage of cells expressing CD2 and CD8α was significantly lower in the IENK than

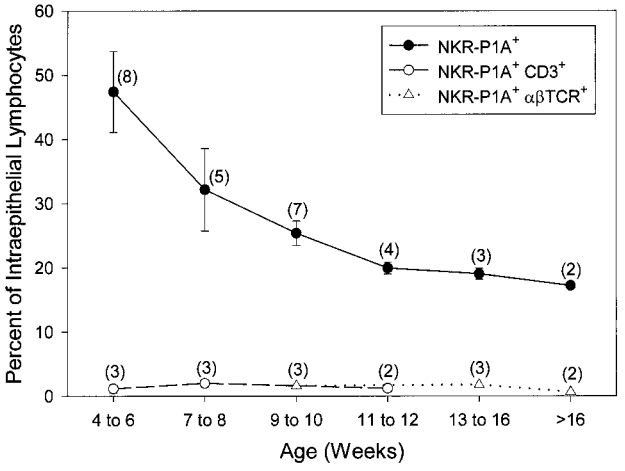

FIGURE 2. Percentage of NKR-P1A$^+$ IEL as a function of age. IEL were isolated from WF rats of either sex at various ages and reacted with either anti-NKR-P1A alone or the combination of anti-NKR-P1A mAb plus either anti-CD3 or anti-$\alpha\beta$-TCR mAb as described in *Materials and Methods*. The percentages of NKR-P1A$^+$, NKR-P1A$^+$CD3$^+$, and NKR-P1A$^+$$\alpha\beta$-TCR$^+$ cells were measured by flow microfluorometry. Each data point represents the mean ± 1 SD; the number of independent measurements for each data point is indicated in parentheses.

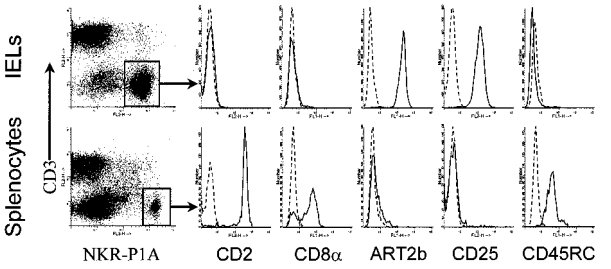

FIGURE 3. Phenotypic analysis of intraepithelial and splenic NK cells. Shown in the *left-most upper* and *lower panels* are representative flow cytometric profiles of NKR-P1A (horizontal axis) and CD3 (vertical axis) staining of IEL (*upper panel*) and splenocytes (*lower panel*) prepared from 7-wk-old WF rats. Cells in the indicated gated regions (NKR-P1A$^+$CD3$^-$) were selected and analyzed for the expression of each indicated Ag. In each of the histograms the intensity of labeling (horizontal axis) is plotted against cell number (vertical axis). Solid lines indicate fluorescence associated with specific staining, and dashed lines indicate fluorescence associated with isotype control Ab staining. The experiment was repeated on cell samples from at least three individual animals, all of which yielded comparable results. The overall dataset for each population is presented in Table I.

in the splenic NK cell population (Table I). In addition we observed several other differences of substantial magnitude. The percentage of cells expressing CD5, CD45RC, and CD54 was also significantly lower in the IENK than in the splenic NK cell population. Conversely, the percentage of cells expressing CD25 and ART2b was significantly higher in the IENK than in the splenic NK cell population. Only CD28 was expressed on similar percentages of IENK and splenic NK cells. Representative histograms documenting the expression of CD2, CD8α, ART2b, CD25, and CD45RC on IENK and splenic NK cells are shown in Fig. 3.

Purified populations of intraepithelial and splenic NK cells are morphologically similar

Because IENK cells differ from splenic NK cells phenotypically, these populations were next purified by flow cytometry as described in *Materials and Methods* and examined for the presence of the azurophilic cytoplasmic granules that are characteristic of peripheral NK cells (11). Light microscopic analysis revealed that nearly all cells in the purified IENK population had the appearance of large granular lymphocytes with azurophilic granules (Fig. 4*A*). These granules were even more prominent than those present in purified splenic NK cells (Fig. 4*B*). Azurophilic granules were absent in the majority of intraepithelial (Fig. 4*C*) and splenic (Fig. 4*D*) T cells.

Both intraepithelial and splenic NK cells lyse NK-sensitive targets

We next measured specific lysis of NK-sensitive YAC-1 cells (12) and NK-resistant C58NT(D) cells (13) in the presence of unfractionated IEL and monocyte-depleted spleen cells. Both IEL and monocyte-depleted spleen cells killed YAC-1, but not C58NT(D), targets (Fig. 5*A*). Flow microfluorometric analysis of the IEL and spleen cell populations in these two experiments revealed that 44–58 and 8–9% of each population, respectively, consisted of NKR-P1A$^+$ cells. Reanalyzing the data in Fig. 5*A* using E:T cell ratios based on these percentages, we found that the specific killing of YAC-1 cells by NKR-P1A$^+$ IENK and splenic NK cells was similar at similar calculated NK to target cell ratios (Fig. 5*B*).

To exclude the possibility that cytotoxic T cells may have contributed to YAC-1 killing by unfractionated IEL, the experiment was repeated using purified populations of NKR-P1A$^+$ and NKR-P1A$^-$ IEL. In this experiment 35% of IEL were NKR-P1A$^+$. We observed that NKR-P1A$^+$ IEL efficiently killed YAC-1 targets, whereas NKR-P1A$^-$ IEL did not (Fig. 5*C*). In control experiments we observed that unstained, unsorted IEL and stained, unsorted IEL exhibited similar YAC-1 killing activities. Finally, sorted NKR-P1A$^+$ and NKR-P1A$^-$ IEL fractions that were remixed at the presort ratio of 35:65 also exhibited YAC-1 killing at IEL to target ratios comparable to those observed using unsorted IEL (Fig. 5*C*).

IENK cells suppress MLC

Because splenic NK cells are known to suppress MLC (24, 25), we analyzed NK cells of intraepithelial origin for similar capability. In preliminary experiments, unfractionated IEL isolated from 7- to 15-wk-old WF rats were tested for their ability to suppress a one-way allogeneic MLC. We observed that responder cell proliferation to alloantigen was substantially reduced in the presence of IEL at IEL/responder ratios of ~1:10 or greater (Fig. 6*A*). At such

Table I. *Phenotype of intraepithelial and splenic NKR-P1A$^+$ CD3$^-$ lymphocytes*[a]

	CD2 (%)	CD8α (%)	CD5 (%)	CD25 (%)	CD28 (%)	CD45RC (%)	CD54 (%)	ART2 (%)
IELs	1.4 ± 1.0*	9.2 ± 3.8*	1.4 ± 1.8*	95.4 ± 2.5*	0.3 ± 1.3**	0.0 ± 1.9*	53.4 ± 4.0*	96.6 ± 1.5*
Splenocytes	94.5 ± 0.3	73.2 ± 3.8	31.5 ± 2.7	2.0 ± 0.7	15.5 ± 6.0	95.8 ± 1.7	97.6 ± 0.7	9.9 ± 1.0

[a] IELs and splenocytes isolated from 7-wk-old WF rats were reacted with Abs directed against NKR-P1A, CD3, and a third surface Ag, and analyzed by flow cytometry as described in *Materials and Methods*. Fluorescence associated with the isotype control Ab was subtracted. Each data point represents the mean ± 1 SD of three independent experiments. *, $p < 0.001$ versus splenocyte population; **, p = NS (Bonferroni adjusted) versus splenocyte population.

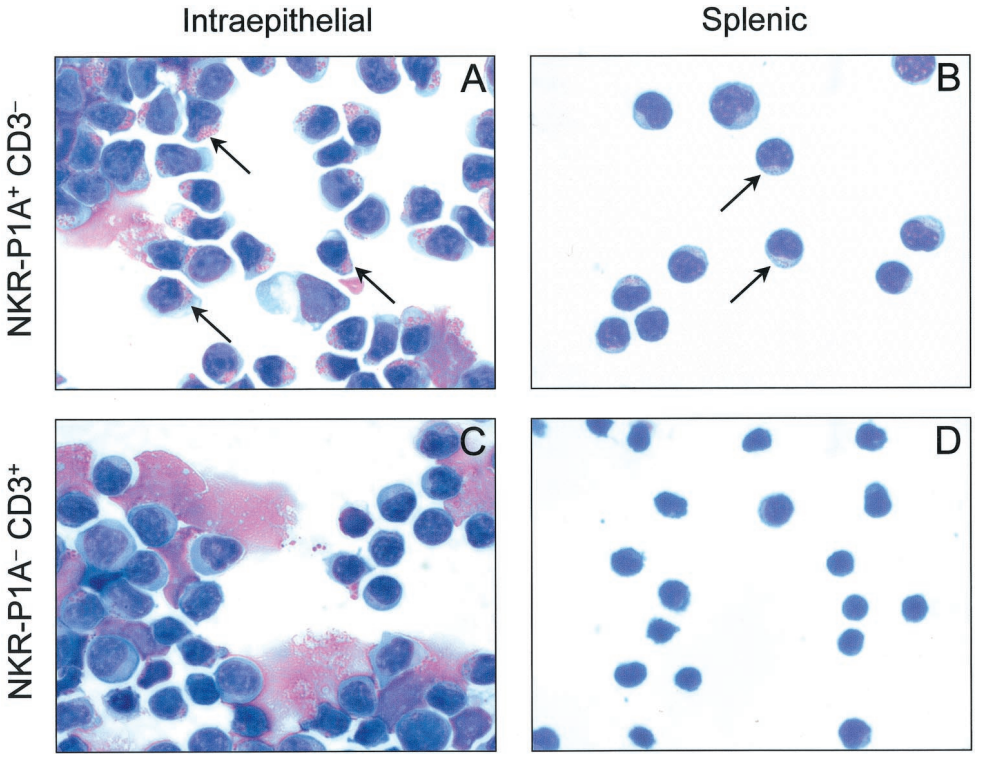

FIGURE 4. Morphology of purified IENK cells and T cells in IEL preparations. IEL (*A* and *C*) and splenocytes (*B* and *D*) were isolated from 4- to 8-wk-old WF rats and sorted into NKR-P1A$^+$CD3$^-$ (*A* and *B*) and NKR-P1A$^-$CD3$^+$ (*C* and *D*) fractions, which were then reacted with Wright-Giemsa stain. Purified NK cells exhibit the morphology of large granular lymphocytes, with abundant azurophilic granules (arrows) present in the cytoplasm (*A* and *B*). Few purified T cells exhibit azurophilic granules (*C* and *D*). Splenic, but not intraepithelial, T cells also appear, in general, to be smaller than splenic NK cells. Magnification, ×100.

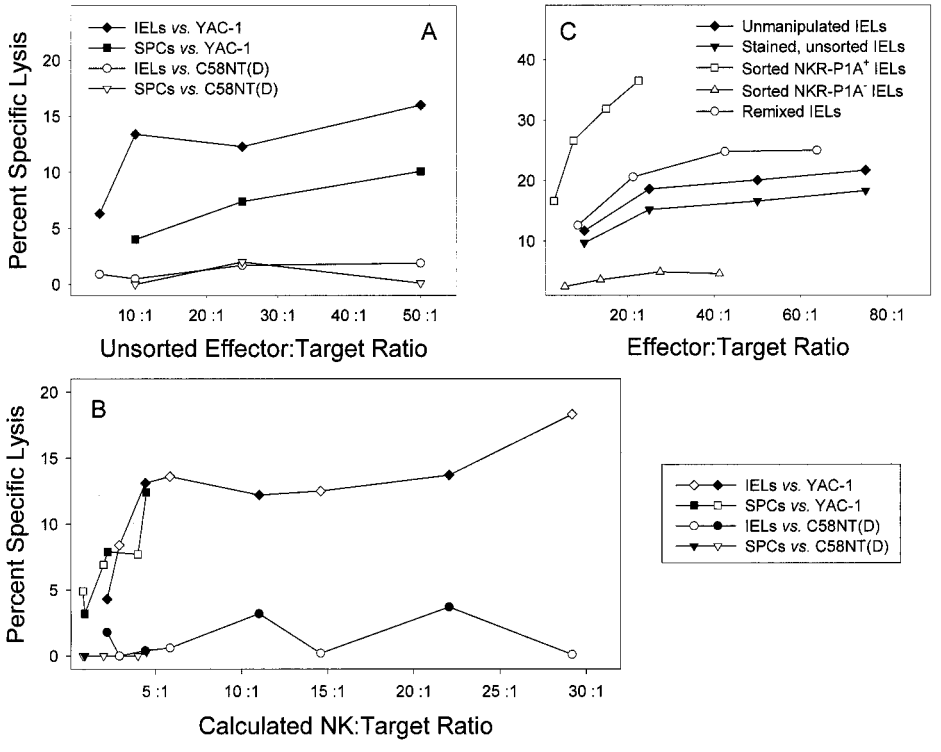

FIGURE 5. Cytotoxic activity of IENK cells. *A*, IEL and monocyte-depleted splenocytes (SPCs) were prepared from WF rats, 5–6 wk of age, and immediately tested for their ability to kill YAC-1 and C58NT(D) cells as described in *Materials and Methods*. Each data point represents the average of two individual experiments, each performed in triplicate. *B*, For both experiments in *A* the percentage of NKR-P1A$^+$ cells in each effector cell population was determined by flow microfluorometry. In those two individual experiments, the percentages of NKR-P1A$^+$ IEL were 59 and 44%, and the percentages of NKR-P1A$^+$ spleen cells were 8 and 9%. These percentages were then used to calculate NK to target cell ratios using the raw data from *A*. Open and filled symbols represent the data from the individual experiments, and each data point represents the mean of a triplicate determination. *C*, IEL were isolated from 6-wk-old WF rats. An aliquot of these cells was not manipulated further. Another aliquot was reacted with anti-NKR-P1A Ab and not manipulated further. A final aliquot was reacted with anti-NKR-P1A Ab and then fractionated by flow microfluorometry. A final population of effector cells was generated by remixing sorted NKR-P1A$^+$ and NKR-P1A$^-$ cell populations at the 35:65 ratio of the presort IEL preparation. Each cell population was tested for its ability to kill YAC-1 cells. Each data point represents the mean of a single experiment performed in triplicate. The experiment was repeated a second time with similar results.

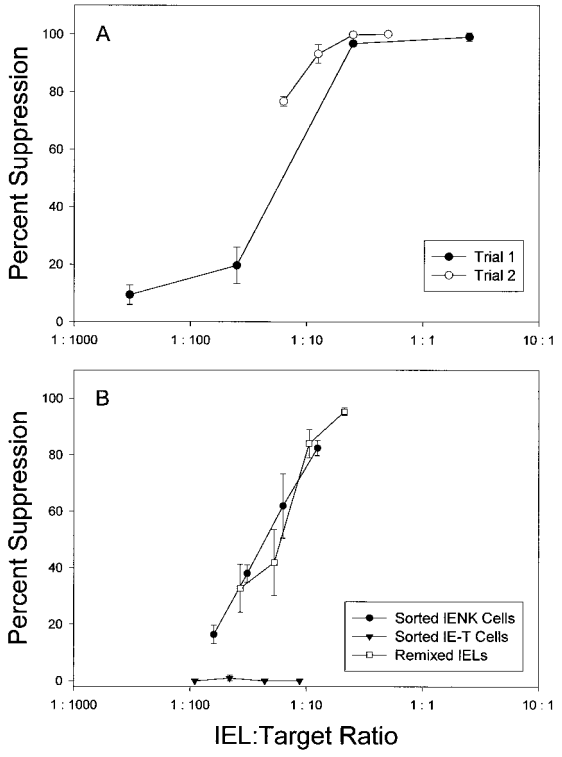

FIGURE 6. Suppressor cell activity of IEL. *A*, IEL were isolated from WF rats 7–15 wk of age and immediately tested for their ability to suppress a one-way MLC as described in *Materials and Methods*. Responder cells were WF MLN cells. Stimulator cells were thymocytes from either syngeneic WF rats or allogeneic DA (filled symbols) or BN (open symbols) rats. Shown are the results of two individual experiments. The absolute counts per minutes (mean ± SEM of triplicate determinations) associated with positive control allogeneic MLCs performed in the absence of IEL was $4.2 \pm 0.3 \times 10^4$ for trial 1 and $8.5 \pm 0.3 \times 10^4$ for trial 2. The cpm for negative control syngeneic MLCs was $0.2 \pm 0.0 \times 10^4$ in both trials. *B*, IEL were isolated from 5- to 7-wk-old WF rats, reacted with anti-NKR-P1A and anti-CD3 Abs, and fractionated into NKR-P1A$^+$CD3$^-$ IENK and NKR-P1A$^-$CD3$^+$ IE-T cell populations by flow microfluorometry. The purity of each fractionated subpopulation was >95%. For the assay of remixed cells, the ratio of IENK to IE-T cells was 3:2, approximately the same as that in the presort IEL preparation. The data shown in *B* represent the result of a single experiment performed using BN allogeneic stimulator cells; comparable results were obtained in a second independent trial using DA allogeneic stimulator cells. The absolute counts per minute for allogeneic and syngeneic MLCs performed in the absence of IEL were $9.2 \pm 0.5 \times 10^4$ and $0.1 \pm 0.0 \times 10^4$, respectively. Each data point in both panels represents the mean percent suppression of a triplicate assay ± SEM, calculated as described in *Materials and Methods*. There were no differences in outcome as a function of the strain of the stimulator cell donor (DA or BN).

ratios, proliferation was reduced to levels observed in control experiments using syngeneic stimulator cells. In additional control experiments, responder cells did not proliferate in the presence of IEL alone, nor did IEL proliferate in the presence of allogeneic stimulator cells alone (data not shown).

Having demonstrated that IEL can suppress a one-way MLC, we next sought to determine which subpopulation of IEL was responsible for the effect. IEL from WF rats were fractionated into NKR-P1A$^+$CD3$^-$ IENK and NKR-P1A$^-$CD3$^+$ intraepithelial T cell (IE-T cell) subpopulations, and their abilities to suppress alloreactive T cell proliferation were compared. As shown in Fig. 6*B*, the suppressive activity of sorted IEL appeared to be restricted exclusively to the IENK subpopulation. There was no suppressive activity associated with sorted IE-T cells. The suppressive activity of

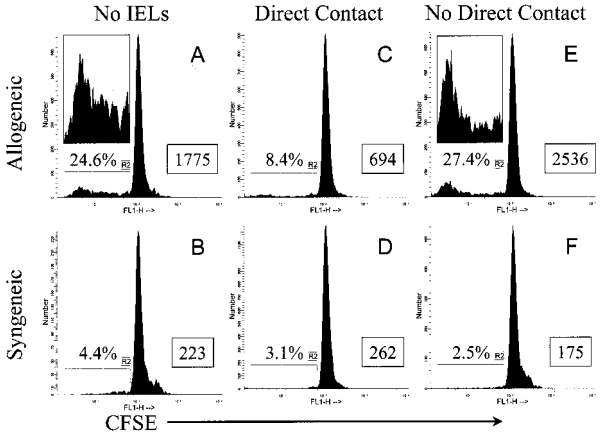

FIGURE 7. Suppressor cell activity of IEL. A one-way MLC was performed using a Transwell apparatus as described in *Materials and Methods*. IEL were isolated from 5- to 7-wk-old WF rats. WF responder cells were labeled with CFSE, and WF syngeneic and DA allogeneic stimulator cells were prepared as described in *Materials and Methods*. The IEL/responder cell ratio was 1:5. Cells were harvested after 5 days of culture, and the intensity of CFSE labeling in the recovered cell population was determined by flow microfluorometry using a lymphocyte gate. The overall percentage of responder cells with reduced CFSE fluorescence, indicative of proliferation, is indicated for each experimental condition. In addition, the absolute number of mitotic events that had occurred per 10^4 responder cells in the analysis was estimated by the method of Wells et al. (17); these calculated numbers are shown in rectangles in each panel. In the absence of IEL, as expected, proliferation of allogeneic, but not syngeneic, responder cells was observed (*A* and *B*). When IEL were incubated with responder and stimulator cells on the same side of the Transwell membrane, the proliferation of allogeneic responder cells was reduced to a level comparable to that observed for syngeneic responder cells (*C* and *D*). In contrast, when IEL were separated from responder and stimulator cells by the Transwell membrane, the proliferation of allogeneic responder cells (*E* and *F*) was similar to that observed in the absence of IEL (*A* and *B*). The two insets present magnified views of the low intensity CFSE gate demonstrating periodic peaks of labeling, consistent with waves of proliferation as previously described (16). Shown are the results of one of two experiments using different IEL preparations that yielded similar results.

sorted IENK and IE-T cells that were subsequently remixed was comparable to those of both sorted IENK cells alone (Fig. 6*B*) and unsorted IEL (Fig. 6*A*).

Having demonstrated that NKR-P1A$^+$CD3$^-$ (IENK) cells are responsible for IEL-mediated suppression of a one-way MLC, we next sought to determine whether a soluble mediator or cell-to-cell contact was more likely to be responsible for this effect. In this experiment MLC was performed using Transwell methodology, and the proliferation of CFSE-labeled responder cells in contact with unfractionated IEL was compared with the proliferation of responder cells separated from IEL by a permeable membrane. As shown in Fig. 7, retention of fluorescence, indicative of suppression, occurred when responder cells, allogeneic stimulator cells, and IEL were incubated on the same side of the Transwell membrane. Loss of fluorescence, indicative of responder cell proliferation and an increase in the absolute number of mitotic events, occurred when responder cells and allogeneic stimulator cells were separated from IEL by the membrane.

IENK cells spontaneously produce IFN-γ and IL-4

To investigate the possible immunoregulatory role of IENK cells, we measured their secretion of IFN-γ and IL-4 using ELISPOT methodology. In a preliminary experiment IEL were isolated from 5- to 11-wk-old WF rats and incubated overnight in the presence

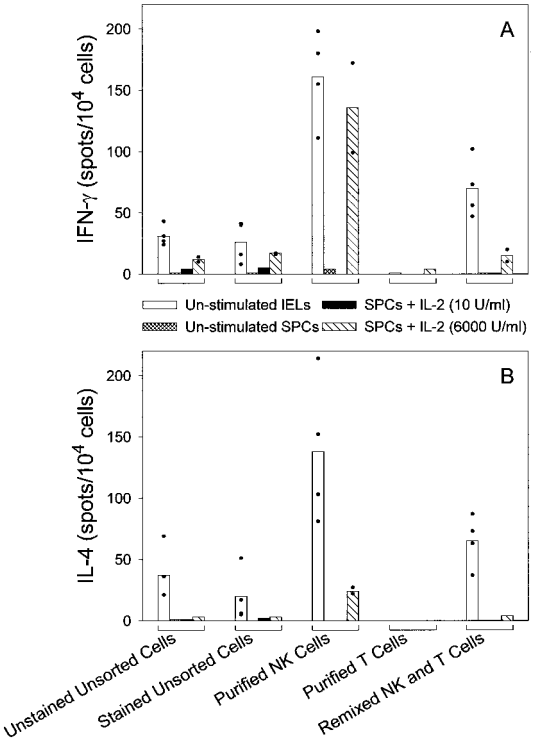

FIGURE 8. IENK cells spontaneously produce IFN-γ and IL-4. IEL and splenocytes (SPCs) were isolated from 4- to 8-wk-old WF rats as described in *Materials and Methods*. Pools of IEL from 8–10 donors and splenocytes from two donors were processed to generate five populations for assay. One aliquot of cells of each type (unstained unsorted cells) was not further manipulated. The remaining cells were reacted with anti-NKR-P1A and anti-CD3 Abs; one aliquot of these (stained unsorted cells) was not further manipulated, and the remaining cells were fractionated by flow microfluorometry into NK cell (purified NK cells) and T cell (purified T cells) populations. A final population of cells (remixed NK and T cells) was prepared from aliquots of fractionated NK and T cells that were remixed at the same ratio as that determined by flow microfluorometry to have been present in the presort cell preparation. IEL samples (□) were incubated overnight in the absence of any in vitro stimulation. Splenocyte samples were incubated in the presence of 0 (▨), 10 (■), or 6000 (▧) U/ml of IL-2. Each preparation of sorted, unsorted, and remixed cells was then assayed in triplicate for the presence of IFN-γ (*A*) or IL-4 (*B*) by ELISPOT as described in *Materials and Methods*, and data are reported as spots per 10^4 cells added to the assay. The analysis of IEL was repeated four times, including two assays that were also used to generate the additional data shown in Fig. 9. The analysis of all other cell populations was repeated twice. Each bar represents the average of the two or four independent trials. In the case of data points with values greater than about 10 spots/10^4 cells, markers (●) indicate the actual values obtained in the trials.

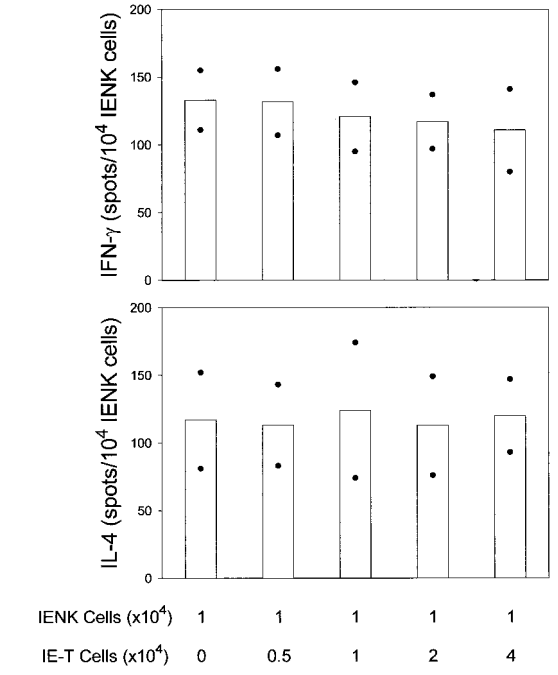

FIGURE 9. The presence of IE-T cells does not affect spontaneous production of IFN-γ and IL-4 by IENK cells. Purified populations of IENK and IE-T cells were prepared from 8–10 WF rats (4- to 8-wk old) by flow microfluorometry as described in *Materials and Methods*. Graded numbers of purified IE-T cells were added to a constant number of purified IENK cells as indicated, and each cell mixture was assayed in triplicate by ELISPOT to quantify the number of cells secreting IFN-γ (*A*) or IL-4 (*B*). Data are reported as spots per 10^4 IENK cells added to the assay. The experiment was performed twice; markers (●) indicate the values obtained in each trial, and bars indicate the average value.

of PMA/ionomycin or IL-2 (10 U/ml). We observed that the frequencies of IFN-γ-secreting IEL under these conditions of stimulation were 25 and 45 spots/10^4 cells, respectively. However, in three separate assays, the frequencies of cells secreting IFN-γ in the absence of any in vitro stimulating agent were comparable: 33, 43, and 23 spots/10^4 cells. The results for IL-4 in this same experiment were similar. PMA/ionomycin- and IL-2-stimulated cells generated 22 and 55 spots/10^4 cells, respectively, and cells cultured in the absence of in vitro stimulation yielded 35, 39, and 46 IL-4 spots/10^4 cells.

We next tested the hypothesis that IENK cells spontaneously secrete IFN-γ and IL-4 and were the source of these cytokines in our preliminary experiment. Because the secretion of IL-4 has not previously been associated with peripheral NK cells, populations of spleen cells were assayed in parallel with cells of intestinal origin. As shown in Fig. 8, we confirmed by ELISPOT that the frequency of unstimulated IEL that produced either IFN-γ or IL-4 was substantial. In contrast, few unstimulated splenocytes produced IFN-γ, and none appeared to produce IL-4. Addition of up to 6000 U/ml IL-2 to these cultures resulted in only a modest increase in the frequency of cells that secreted IFN-γ and no increase in the number of cells that secreted IL-4.

Analysis of sorted populations of IENK and IE-T cells localized the production of both IFN-γ and IL-4 by IEL to the IENK subpopulation (Fig. 8). Additional assays confirmed that unstimulated splenic NK and T cells did not spontaneously secrete IL-4, and only a few secreted IFN-γ. Addition of 10 U/ml IL-2 to the splenic NK cell cultures had little effect on the number of cells that produced either cytokine. When 6000 U/ml was added to the splenic NK cell cultures, the frequency of cells that produced IFN-γ rose to levels comparable to those observed for unstimulated IENK cells, but the number of cells that produced IL-4 remained low. The frequency of sorted intraepithelial and splenic T cells that secreted IFN-γ was small, and no cells that secreted IL-4 were detectable. Comparable and consistent results were obtained in control assays of stained, unsorted cells and a remixed population of sorted NK and T cells (Fig. 8).

To exclude further any possibility that contaminating IE-T cells may have been responsible for the cytokine production attributed to the IENK population, an additional ELISPOT assay was conducted. In this assay graded numbers of purified IE-T cells were added to a constant number of purified IENK cells, and the number of IFN-γ- and IL-4-producing cells was measured as described above. As shown in Fig. 9, there was no detectable change in the

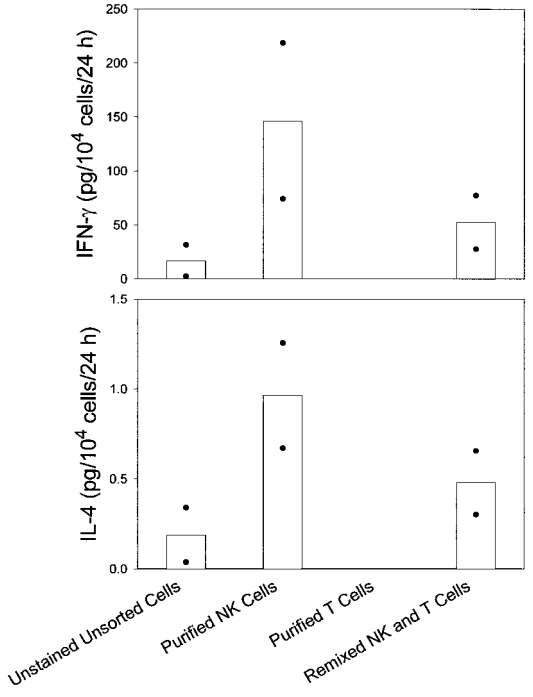

FIGURE 10. IFN-γ and IL-4 production by unstimulated IENK cells. Purified IENK and IE-T cells were prepared from 8–10 WF rats (4- to 8-wk old) as described in *Materials and Methods*. Unsorted, sorted, and remixed populations were incubated overnight in the absence of any in vitro stimulation. The amounts of IFN-γ (*A*) and IL-4 (*B*) secreted by each preparation were then quantified by cell-ELISA as described in *Materials and Methods*. Data are reported as picograms of cytokine produced per 10^4 cells per 24 h. The experiment was performed twice; markers (●) indicate the values obtained in each trial, and bars indicate the average value.

number of cytokine-producing cells as a function of the number of IE-T cells that were added to the IENK cells. In each experimental condition the number of cytokine-positive cells, when expressed as positive cells per 10^4 IENK cells in the assay, remained constant.

Quantification of IFN-γ and IL-4 production by IENK cells

Having quantified the number of IENK cells that produced IFN-γ and IL-4 spontaneously, we next sought to determine the amount of cytokine produced. To circumvent the problem of reuse of cytokines inherent in such determinations, we developed the modified cell-ELISA (20) described in *Materials and Methods*. As shown in Fig. 10, we again confirmed that unstimulated IEL and IENK cells, but not IE-T cells, produce readily detectable quantities of both IFN-γ and IL-4. IENK cells produced IFN-γ at a rate of ~150 pg/10^4 cells/24 h and IL-4 at a rate of ~1 pg/10^4 cells/24 h. Results for unsorted and remixed IEL gave consistent results based on the fraction of IENK cells present in these populations.

Discussion

Using new methodology we have identified a novel population of IENK cells that appear constitutively to secrete IL-4 and IFN-γ. These unusual IENK cells are similar to peripheral NK cells in morphology, in their ability to lyse NK-specific targets, and in their ability to suppress a one-way MLC. However, they are markedly different from peripheral NK cells in two respects. First, IENK cells express high levels of CD25 and ART2, whereas peripheral NK cells do not. Second, unlike splenic NK cells that secrete little or no IL-4 and secrete IFN-γ only in response to stimulation (26), a substantial fraction of rat IENK cells appear to secrete IFN-γ or IL-4 spontaneously.

We (8) and others (23) have previously reported that cells with an NKR-P1A$^+$CD3$^-$ phenotype are present in the intraepithelial compartment of the rat intestine. Our data now extend these observations by demonstrating that IENK cells appear to represent a new, previously unrecognized subpopulation of rat NK cells. It could, of course, be argued that the IL-4 secretion we observed in rat IENK cell populations resulted from contamination of the IENK cell preparation with either NK T cells or contaminating IE-T cells, both of which are known to secrete IL-4 (6, 27). However, this is unlikely because our assays revealed that NK T and IE-T cells comprised <0.1% of the purified IENK cell preparations used in our ELISPOT assays. This frequency of contaminating cells is insufficient to account for the 1–2% frequency of IL-4-secreting cells we observed in the purified IENK populations. In addition, we observed that the purposeful addition of IE-T cells to the IENK ELISPOT had no effect on the number of cytokine-secreting cells.

It could also be argued that the apparently spontaneous secretion of IL-4 was simply the result of the IENK cells being activated, as are nearly all IELs (6, 28). However, this is also unlikely because our data show clearly that peripheral NK cells, even when activated with high levels of IL-2, secrete little IL-4. The ability of freshly isolated IENK cells to secrete IL-4 suggests that these cells may represent a new subpopulation of NK cells that, in the microenvironment of the IEL compartment, are programmed to secrete IL-4 constitutively. However, it should be pointed out that our data do not formally exclude the possibility that factors other than IL-2 or IL-4 could be present in vivo in the gut, activate IENK cells, and induce them to secrete IL-4. Whether any individual IENK cells secrete both IFN-γ and IL-4 spontaneously also cannot be determined from our data.

Consistent with the view that IENK cells comprise a distinct NK subpopulation is our documentation that they differ phenotypically from splenic NK cells. Expression of CD2, CD8α, CD5, CD45RC, and CD54 is lower in intraepithelial than in splenic NK cell populations. In contrast, expression of CD25 and ART2 is higher. Although the expression of CD25 could simply reflect the constitutively activated state of IENK cells, ART2 expression on peripheral T cells is known to be down-regulated in the setting of activation (29).

Although the cytokine profile of rat IENK cells appears to be unique among cells with the NKR-P1A$^+$CD3$^-$ phenotype, it is important to note that these cells do share important morphological and functional characteristics with peripheral NK cells. Both are large and exhibit distinctive azurophilic granules (30). We recognize that γδ-TCR$^+$ IEL have been reported to have azurophilic granules (31), but this cell subset was excluded from the IENK cell specimens that we analyzed. Our morphological studies also suggest that IENK cells may be slightly larger than those in the splenic population, consistent with their activated state (26). However, this conclusion must be regarded as tentative as we cannot exclude the possibility of artifact induced by the cytospin method used for specimen preparation.

We also observed that, like peripheral NK cells (11, 12, 24, 25), IENK cells exhibit cytotoxic activity and suppress a one-way MLC. The cytotoxicity data, which showed that purified rat NKR-P1A$^+$ IEL lyse YAC-1 cells more efficiently than do unsorted or remixed populations, are consistent with studies performed using mouse spleen cells (30). We recognize that NK T cells were present in our cytotoxicity assays, but it is unlikely that they affected the outcome because, unless they are preincubated in the presence of high dose IL-2, NK T cells are ineffective in lysing YAC-1 cells (27). With respect to the suppression of MLCs by rat IENK cells, it should be pointed out that comparable numbers of

IE-T cells did not result in suppression, arguing against competition for nutrients in the medium as a mechanism of suppression. NK-mediated suppression of a one-way MLC is thought to occur via killing of allogeneic APC (24, 25), a conclusion supported by our Transwell studies. These studies suggest that cell-cell contact between IENK and stimulator/responder cells may be required for suppression, but it must be recognized that they do not formally exclude the possibility that soluble mediators that are either short-lived or present at low concentrations could be involved.

The constellation of NK-like phenotype and function together with an unusual cytokine profile, i.e., constitutive expression of IL-4 and IFN-γ in the local microenvironment of the gut, suggest that these are specialized cells that may be subserving a gut-specific function. If the IENK cell population is indeed a new subpopulation of intraepithelial cells, how might they influence gut immunity? We propose that IENK cells have previously unrecognized regulatory properties. The gut is known to exhibit unique immune responses that differ from those in the systemic circulation and can influence the response of the peripheral immune system (1).

Two unique immune responses mediated by the gut are regulation of controlled or physiologic inflammation (1), and mediation of oral tolerance upon encounter with exogenous Ags (1, 6, 28, 32). The ability of IENK cells to spontaneously (in essence, constitutively) secrete IL-4 implies an important role vis-à-vis these two unique functions of the gut immune system. IL-4 is known to be a potent regulator of inflammatory processes and biases inflammation toward a nondestructive rather than a proinflammatory destructive process (33–35). IL-4 has also been demonstrated to protect animals from inflammatory bowel disease (3), and it is required for oral tolerance (36). Interestingly, NKR-P1$^+$ cell populations have been implicated in the regulation of a Th1-type immune response in a mouse model of chronic colitis, but it is not known specifically whether NK cells of gut origin subserve that function (37).

With regard to possible immunoregulatory function, it is intriguing to note that ART2 (29) and CD25 are expressed at high levels on rat IENK cells. Expression of ART2 on peripheral rat T cells is a marker of regulatory capability (29, 38), as is expression of CD25 on a population of peripheral mouse T cells that can prevent autoimmune diabetes in NOD mice (39). It is plausible to speculate that ART2$^+$CD25$^+$ rat IENK cells could play a role in the processes that regulate the physiologic inflammation that is characteristic of the gut (1).

Our data suggest further that defects in IENK cell number or function might lead to unregulated inflammatory processes in the gut that result in disease. Abnormalities in gut immunity may participate in the pathogenesis of autoimmune disorders, including celiac disease (2), inflammatory bowel diseases (3–5), and autoimmune type 1 diabetes (32). With respect to diabetes, we have documented that the spontaneously diabetic, diabetes-prone BB rat strain of rats is severely deficient in IENK cells (D. J. Todd, unpublished observations). The diabetes-resistant BB rat strain is also deficient in IENK cells compared with the normal WF strain rat used in the present studies. Interestingly, however, when diabetes-resistant BB rat are induced to become diabetic using a standard protocol consisting of anti-ART2 mAb plus polyinosinic-polycytidylic acid (40), levels of IENK cells become nearly undetectable (D. J. Todd, unpublished observations).

There is as yet little information on the abundance and function of IENK cells in species other than the rat. Some IEL in both human and mouse express NK cell surface markers (41–43), and mouse IEL exhibit NK-like cytotoxic activity (41, 44). However, most IEL in mice (6) and humans (45) are CD3$^+$, and spontaneous secretion of IFN-γ (and IL-5) in the mouse has been associated with intraepithelial CD3$^+$ T cell populations (46).

In conclusion, we have demonstrated that the rat IEL compartment harbors a large population of NKR-P1A$^+$CD3$^-$ cells that function as NK cells, but display an activated phenotype and highly unusual cytokine profile that clearly distinguish them from splenic NK cells. Their phenotypic and functional characteristics suggest that these distinctive IENK cells may participate in the regulation of mucosal immunity.

Acknowledgments

We thank Dr. Bruce Woda for assistance with the interpretation of histology specimens, and Lisa Burzenski, Kelly Lake, and Michael Bates for technical assistance.

References

1. Mayer, L. 2000. Mucosal immunity and gastrointestinal antigen processing. *J. Pediatr. Gastroenterol. Nutr. 30(Suppl):S4.*
2. Schuppan, D. 2000. Current concepts of celiac disease pathogenesis. *Gastroenterology 119:234.*
3. Groux, H., and F. Powrie. 1999. Regulatory T cells and inflammatory bowel disease. *Immunol. Today 20:442.*
4. Mayer, L. 2000. IBD: immunologic research at the Mount Sinai Hospital. *Mt. Sinai J. Med. 67:208.*
5. Mayer, L. 2000. The development of animal models of inflammatory bowel disease. *Int. Rev. Immunol. 19:77.*
6. Beagley, K. W., and A. J. Husband. 1998. Intraepithelial lymphocytes: origins, distribution, and function. *Crit. Rev. Immunol. 18:237.*
7. Campbell, N., X. Y. Yio, L. P. So, Y. Li, and L. Mayer. 1999. The intestinal epithelial cell: processing and presentation of antigen to the mucosal immune system. *Immunol. Rev. 172:315.*
8. Todd, D., A. J. Singh, D. L. Greiner, J. P. Mordes, A. A. Rossini, and R. Bortell. 1999. A new isolation method for rat intraepithelial lymphocytes. *J. Immunol. Methods 224:111.*
9. Bayer, E., and M. Wilcheck. 1974. Insolubilized biotin for the purification of avidin. *Methods Enzymol. 34:265.*
10. Iwakoshi, N. N., I. Goldschneider, F. Tausche, J. P. Mordes, A. A. Rossini, and D. L. Greiner. 1998. High frequency apoptosis of recent thymic emigrants in the liver of lymphopenic diabetes prone BioBreeding rats. *J. Immunol. 160:5838.*
11. Woda, B. A., M. L. McFadden, R. M. Welsh, and K. M. Bain. 1984. Separation and isolation of rat natural killer (NK) cells from T cells with monoclonal antibodies. *J. Immunol. 132:2183.*
12. Ortaldo, J. R., R. Winkler-Pickett, A. C. Morgan, C. Woodhouse, R. Kantor, and C. W. Reynolds. 1987. Analysis of rat natural killer cytotoxic factor (NKCF) produced by rat NK cell lines and the production of a murine monoclonal antibody that neutralizes NKCF. *J. Immunol. 139:3159.*
13. Reynolds, C. W., E. W. Bere, Jr., and J. M. Ward. 1984. Natural killer activity in the rat. III. Characterization of transplantable large granular lymphocyte (LGL) leukemias in the F344 rat. *J. Immunol. 132:534.*
14. Markees, T. G., N. E. Phillips, R. J. Noelle, L. D. Shultz, J. P. Mordes, D. L. Greiner, and A. A. Rossini. 1997. Prolonged survival of mouse skin allografts in recipients treated with donor splenocytes and antibody to CD40 ligand. *Transplantation 64:329.*
15. Whalen, B. J., L. C. Love, J. P. Mordes, A. A. Rossini, and D. L. Greiner. 1999. Intravital dye-labeled diabetogenic rat T cells retain dye, home to the pancreas, and induce diabetes. *Transplant. Proc. 31:1611.*
16. Wells, A. D., M. C. Walsh, D. Sankaran, and L. A. Turka. 2000. T cell effector function and anergy avoidance are quantitatively linked to cell division. *J. Immunol. 165:2432.*
17. Wells, A. D., H. Gudmundsdottir, and L. A. Turka. 1997. Following the fate of individual T cells throughout activation and clonal expansion: signals from T cell receptor and CD28 differentially regulate the induction and duration of a proliferative response. *J. Clin. Invest. 100:3173.*
18. Hutchings, P. R., G. Cambridge, J. P. Tite, T. Meager, and A. Cooke. 1989. The detection and enumeration of cytokine-secreting cells in mice and man and the clinical application of these assays. *J. Immunol. Methods 120:1.*
19. van der Meide, P. H., A. M. Joosten, P. Hermans, T. C. Kloosterman, T. Olsson, and M. C. de Labie. 1991. Assessment of the inhibitory effect of immunosuppressive agents on rat T cell interferon-γ production using an ELISPOT assay. *J. Immunol. Methods 144:203.*
20. Ewen, C., and M. E. Baca-Estrada. 2001. Evaluation of interleukin-4 concentration by ELISA is influenced by the consumption of IL-4 by cultured cells. *J. Interferon Cytokine Res. 21:39.*
21. Nie, N. H., C. H. Hull, J. G. Jenkins, K. Steinbrenner, and D. H. Bent. 1975. *Statistical Package for the Social Sciences.* McGraw-Hill, New York, p. 1.
22. O'Brien, P. C., and M. A. Shampo. 1988. Statistical considerations for performing multiple comparisons in a single experiment. II. Comparisons among multiple therapies. *Mayo Clin. Proc. 63:816.*
23. Helgeland, L., J. T. Vaage, B. Rolstad, T. S. Halstensen, T. Midtvedt, and P. Brandtzaeg. 1997. Regional phenotypic specialization of intraepithelial lymphocytes in the rat intestine does not depend on microbial colonization. *Scand. J. Immunol. 46:349.*

24. Shah, P. D., S. M. Gilbertson, and D. A. Rowley. 1985. Dendritic cells that have interacted with antigen are targets for natural killer cells. *J. Exp. Med. 162:625.*
25. Ciccone, E., D. Pende, O. Viale, C. Di Donato, G. Tripodi, A. M. Orengo, J. Guardiola, A. Moretta, and L. Moretta. 1992. Evidence of a natural killer (NK) cell repertoire for (allo) antigen recognition: definition of five distinct NK-determined allospecificities in humans. *J. Exp. Med. 175:709.*
26. Tay, C. H., E. Szomolanyi-Tsuda, and R. M. Welsh. 1998. Control of infections by NK cells. *Curr. Top. Microbiol. Immunol. 230:193.*
27. Bendelac, A., M. N. Rivera, S. H. Park, and J. H. Roark. 1997. Mouse CD1-specific NK1 T cells: development, specificity, and function. *Annu. Rev. Immunol. 15:535.*
28. Hayday, A., and J. L. Viney. 2000. The ins and outs of body surface immunology. *Science 290:97.*
29. Bortell, R., T. Kanaitsuka, L. A. Stevens, J. Moss, J. P. Mordes, A. A. Rossini, and D. L. Greiner. 1999. The RT6 (Art2) family of ADP-ribosyltransferases in rat and mouse. *Mol. Cell. Biochem. 193:61.*
30. Hackett, J., M. Tutt, M. Lipscomb, M. Bennett, G. Koo, and V. Kumar. 1986. Origin and differentiation of natural killer cells. II. Functional and morphologic studies of purified NK-1.1$^+$ cells. *J. Immunol. 136:3124.*
31. Haas, W., P. Pereira, and S. Tonegawa. 1993. γ/δ cells. *Annu. Rev. Immunol 11:637.*
32. Vaarala, O. 2000. The role of the gut in β-cell autoimmunity and type 1 diabetes: a hypothesis. *Pediatr. Diabetes 1:217.*
33. Falcone, M., and N. Sarvetnick. 1999. Cytokines that regulate autoimmune responses. *Curr. Opin. Immunol. 11:670.*
34. Antin, J. H., and J. L. Ferrara. 1992. Cytokine dysregulation and acute graft-versus-host disease. *Blood 80:2964.*
35. Fowell, D., A. J. McKnight, F. Powrie, R. Dyke, and D. Mason. 1991. Subsets of CD4$^+$ T cells and their roles in the induction and prevention of autoimmunity. *Immunol. Rev. 123:37.*
36. Rizzo, L. V., R. A. Morawetz, N. E. Miller-Rivero, R. Choi, B. Wiggert, C. C. Chan, H. C. Morse III, R. B. Nussenblatt, and R. R. Caspi. 1999. IL-4 and IL-10 are both required for the induction of oral tolerance. *J. Immunol. 162:2613.*
37. Fort, M. M., M. W. Leach, and D. M. Rennick. 1998. A role for NK cells as regulators of CD4$^+$ T cells in a transfer model of colitis. *J. Immunol. 161:3256.*
38. Fowell, D., and D. Mason. 1993. Evidence that the T cell repertoire of normal rats contains cells with the potential to cause diabetes: characterization of the CD4$^+$ T cell subset that inhibits this autoimmune potential. *J. Exp. Med. 177:627.*
39. Salomon, B., D. J. Lenschow, L. Rhee, N. Ashourian, B. Singh, A. Sharpe, and J. A. Bluestone. 2000. B7/CD28 costimulation is essential for the homeostasis of the CD4$^+$CD25$^+$ immunoregulatory T cells that control autoimmune diabetes. *Immunity 12:431.*
40. Mordes, J. P., R. Bortell, H. Groen, D. L. Guberski, A. A. Rossini, and D. L. Greiner. 2001. Autoimmune diabetes mellitus in the BB rat. In *Animal Models of Diabetes: A Primer*. A. A. F. Sima and E. Shafrir, eds. Harwood, Amsterdam, p. 1.
41. Carman, P. S., P. B. Ernst, K. L. Rosenthal, D. A. Clark, A. D. Befus, and J. Bienenstock. 1986. Intraepithelial leukocytes contain a unique subpopulation of NK-like cytotoxic cells active in the defense of gut epithelium to enteric murine coronavirus. *J. Immunol. 136:1548.*
42. Eiras, P., F. Leon, C. Camarero, M. Lombardia, E. Roldan, A. Bootello, and G. Roy. 2000. Intestinal intraepithelial lymphocytes contain a CD3$^-$CD7$^+$ subset expressing natural killer markers and a singular pattern of adhesion molecules. *Scand. J. Immunol. 52:1.*
43. Deusch, K., K. Pfeffer, K. Reich, M. Gstettenbauer, S. Daum, F. Luling, and M. Classen. 1991. Phenotypic and functional characterization of human TCR $\gamma\delta^+$ intestinal intraepithelial lymphocytes. *Curr. Top. Microbiol. Immunol. 173: 279.*
44. Tagliabue, A., A. D. Befus, D. A. Clark, and J. Bienenstock. 1982. Characteristics of natural killer cells in the murine intestinal epithelium and lamina propria. *J. Exp. Med. 155:1785.*
45. Ebert, E. C. 1989. Proliferative responses of human intraepithelial lymphocytes to various T-cell stimuli. *Gastroenterology 97:1372.*
46. Taguchi, T., W. K. Aicher, K. Fujihashi, M. Yamamoto, J. R. McGhee, J. A. Bluestone, and H. Kiyono. 1991. Novel function for intestinal intraepithelial lymphocytes: murine CD3$^+$, γ/δ TCR$^+$ T cells produce IFN-γ and IL-5. *J. Immunol. 147:3736.*